

Acid–Base Equilibrium and Electron-Ejection Processes in the Excited States of *N,N*-Dimethyl-1-aminonaphthalene in Aqueous Solution

So Tajima, Seiji Tobita,* and Haruo Shizuka

Department of Chemistry, Gunma University, Kiryu, Gunma 376-8515, Japan

Received: February 7, 2000; In Final Form: May 4, 2000

Acid–base equilibrium and photoinduced electron-ejection processes of *N,N*-dimethyl-1-aminonaphthalene (DMAN) in aqueous solution have been investigated by nanosecond laser photolysis and fluorescence measurements. Depending on the different pK_a values for the ground ($pK_a(S_0) = 4.6$), lowest excited singlet ($pK_a(S_1) = 2.5$), and triplet ($pK_a(T_1) = 2.7$) states, photoionization pathways varied with acidity of solution. Upon 266 nm laser excitation, the direct electron-ejection took place from the S_1 state of DMAN in aqueous solution at $pH > \sim 6.0$, which was revealed to occur from the nonrelaxed S_1 state. At $pH 2.0$ – 4.0 , proton dissociation took place in the S_1 state of $DMANH^+$ (protonated DMAN), which was followed by electron-ejection to produce $DMAN^{+\bullet}$. In addition to the above ionization processes, a slow electron-ejection process was found to occur from the T_1 state of DMAN. The possible photoionization mechanisms of aqueous DMAN are discussed on the basis of kinetic analyses, thermochemical considerations, and electronic structures.

1. Introduction

We have recently investigated photoionization (photoelectron-ejection) of aromatic compounds in aqueous solution by means of the laser photolysis method and fluorescence measurements. For aniline and its derivatives in aqueous solution^{1,2} it has been revealed that the ionization took place from nonrelaxed S_1 state by one-photon absorption at 266 nm. For 1,4-dimethoxybenzene (DMB) in aqueous solution,^{3,4} a dominant photoionization mechanism has been found to be electron-ejection to solvent by two-photon absorption at 266 nm. Furthermore, it has been revealed that electron transfer (ET) from excited triplet DMB ($^3DMB^*$) to hydronium ion was involved under acidic conditions.⁴ The latter process also resulted in formation of the solute cation radical, though the rate was much slower compared to the direct photoelectron ejection.

Photophysics of aromatic amines in aqueous solution is characterized by not only its feasibility of photoelectron ejection as described above but also proton exchange with solvent, i.e., acid–base reactions.^{5–8} The latter process can be observed both in the ground and excited states. Since the rate of proton dissociation and association is strongly dependent on the electronic structure of solute molecules, acid–base property in the excited states is usually modified significantly compared to that in the ground state.^{5–8}

In proton exchange and electron-ejection processes, the role of solvent is considered to be a key factor to determine their efficiencies. Both processes are associated with interactions between an excited aromatic amine (RNH_2) and water molecules as shown in the following equations:



In proton dissociation reactions from excited protonated amines

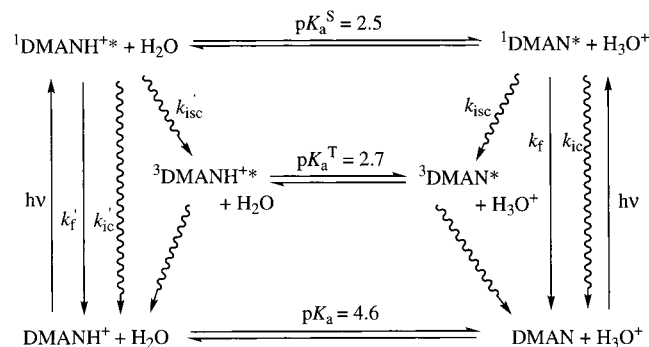
(RNH_3^+), the ejected proton is stabilized by hydration to produce a hydronium ion. Solvation change of the solute molecule occurring with the proton ejection also affects the relative stability between reactants and products. Similarly the electron-ejection process results in the solute cation radical ($\text{RNH}_2^{+\bullet}$) and hydrated electron (e_{aq}^-) which are stabilized by solvation in water.

As a typical compound showing acid–base reactions in both ground and excited states, the photochemistry of *N,N*-dimethyl-1-aminonaphthalene (DMAN) in aqueous solution^{5,7,9} has been studied. In addition, detailed photophysical properties of this compound in various organic solvents have been reported.^{10–13} As an important factor to determine the photophysical properties, the internal twisting coordinate of the dimethylamino group with respect to the naphthalene ring has been invoked.^{11–13} The conformation of the amino group of DMAN is pretwisted in the ground state, while in the fluorescent state the conformation is relaxed to a more planar structure, which facilitates intramolecular charge transfer (ICT) from the amino group to the naphthalene moiety. Such a conformational change of the amino group and ICT character in the S_1 state of DMAN are related to a decrease in the pK_a value from 4.6 (S_0) to 2.5 (S_1).^{5,7} Acid–base equilibria of DMAN in the ground (S_0) and lowest excited singlet (S_1) and triplet (T_1) states are shown in Scheme 1.

In the present paper, the electron-ejection processes of excited DMAN in aqueous solution together with those of the proton dissociation and association reactions were investigated by means of laser flash photolysis and fluorescence spectroscopy. It was found that the photoionization processes of DMAN were quite different from those of DMB.⁴ Three different types of electron photoejection mechanisms, (1) the direct photoionization of DMAN, (2) proton dissociation of $DMANH^+$ (protonated DMAN) followed by electron-ejection in the S_1 state, and (3) slow electron ejection from triplet DMAN are discussed from the viewpoints of thermochemical considerations and stabilization by solvation of the reaction products.

* Corresponding author. Phone: 81-277-30-1210. Fax: 81-277-30-1213. E-mail: tobita@chem.gunma-u.ac.jp.

SCHEME 1



2. Experimental Section

Materials. *N,N*-Dimethyl-1-aminonaphthalene (DMAN) (Wako) and aniline (Kanto) were purified by vacuum distillation. Naphthalene (Np) (Wako) was purified by vacuum sublimation. Quinine bisulfate (Wako) was recrystallized from water. Potassium hexacyanoferrate(II), 3-hydrate (KISHIDA, 99.5%) was used without further purification. Deionized water was purified by using a Millipore MILLI-Q-Labo. Cyclohexane (CH) (Aldrich, spectrophotometric grade) was treated on an alumina column prior to use. Ethanol, methanol, and acetonitrile (ACN) were purified by distillation. H₂SO₄ (Wako, 97%, S. S. Grade), KOH (Kanto), and Cs₂SO₄ (Fluka, 99.9%) were used as received. The concentration of H₃O⁺ of each aqueous solution was determined by a pH meter (Horiba F-8) calibrated at pH 4.00 (phthalate pH standard solution (Wako)), pH 6.88 (phosphate pH standard equimolar solution (Wako)), and pH 9.22 (tetraborate pH standard solution (Wako)) at 293 K. H₂SO₄ and KOH were used to adjust the hydronium ion concentration ([H₃O⁺]) of sample solutions.

The concentration of DMAN and DMANH⁺ in each solution was maintained at 2.3 × 10⁻⁴ M and 1.1 × 10⁻⁴ M for laser experiments and 3.8 × 10⁻⁵ M and 1.8 × 10⁻⁵ M for fluorescence ones, respectively. All sample solutions in a quartz cell with a 10-mm optical path length were thoroughly degassed by freeze-pump-thaw cycles on a high-vacuum line.

Methods. The absorption and fluorescence spectra were measured with a UV/vis spectrophotometer (JASCO, Ubest-50) and a spectrofluorometer (Hitachi, F-4010), respectively. The fluorescence lifetime (τ_f) was obtained with a time-correlated single-photon-counting fluorometer (Edinburgh Analytical Instruments, FL900CDT). A nanosecond pulsed discharge lamp (pulse width ~1.0 ns, repetition rate 40 kHz) filled with hydrogen gas was used as the excitation light source. This apparatus enabled us to measure both excitation and emission response functions, and to compute decay parameters by the deconvolution method using a nonlinear least-squares fitting.

The nanosecond laser flash photolysis experiments were carried out by using the fourth harmonics (266 nm) of a Nd³⁺:YAG laser (Spectra-Physics GCR-130, pulse width 6 ns) as the excitation source. The monitoring system of transient species consisted of a pulsed xenon lamp (Ushio, UXL-151D), a monochromator (Ritsu, MC-20N), and a photomultiplier (Hamamatsu, R928). The timing sequence between the laser pulse and the xenon flash lamp was controlled by a digital delay pulse generator (Stanford Research Systems, Model DG-535). The transient signals were recorded on a digitizing oscilloscope (Tektronix, TDS-744; 500 MHz, 2 × 10⁹ samples s⁻¹) and transferred to a personal computer (NEC, PC-9821Ap) to analyze the data. The signals were averaged over 5–20 laser shots to improve the signal-to-noise ratio. The laser power

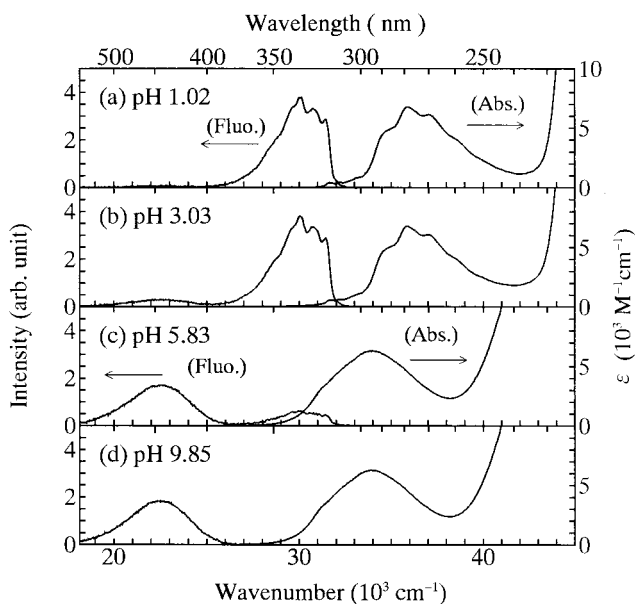


Figure 1. Absorption (Abs.) and fluorescence (Fluo.) spectra of DMAN in aqueous solutions with different pH values at 293 K. The fluorescence spectra were obtained upon 266 nm excitation.

each shot was monitored by a pyroelectric detector (Scientech, P25/S200). All sample solutions were exposed to less than 100 laser shots to avoid depletion of the starting materials and accumulation of possible photoproducts.

The fluorescence quantum yields (Φ_f) of DMAN and DMANH⁺ were determined by using quinine bisulfate in 1 N H₂SO₄ solution ($\Phi_f = 0.546$)¹⁴ and aniline in CH ($\Phi_f = 0.17$)¹⁵ as standards, respectively. The quantum yields for the formation of ³DMAN* ($\epsilon = 5100 \text{ M}^{-1} \text{ cm}^{-1}$ at 550 nm)⁹ and DMAN* ($\epsilon = 1370 \text{ M}^{-1} \text{ cm}^{-1}$ at 700 nm)⁹ were determined by using Np in CH ($\Phi_{isc} = 0.75$ ¹⁶ and $\epsilon = 24500 \text{ M}^{-1} \text{ cm}^{-1}$ at 415 nm¹⁷) as an actinometer.

3. Results and Discussion

3.1. Spectral Properties of DMAN in Aqueous Solutions with Different pH Values. Figure 1 shows the absorption and fluorescence spectra of DMAN in aqueous solution with different pH values at 293 K. The pK_a values of the ground (*S*₀) and excited singlet (*S*₁) states of DMAN have been reported to be 4.6 and 2.5,⁷ respectively (Scheme 1). At pH 1.02 (Figure 1a), the spectral features of the absorption and fluorescence bands are similar to those of 1-methylnaphthalene;¹⁸ the first absorption band (*S*₁(¹L_b) ← *S*₀(¹A)) appears at 31500 cm⁻¹ and the second absorption band (*S*₁(¹L_a) ← *S*₀(¹A)) at 34400 cm⁻¹.¹⁹ This indicates that most of the DMAN molecules are protonated at the nitrogen atom both in the *S*₀ and *S*₁ states under this condition. At pH 5.83, ca. 6% of DMAN is protonated in the *S*₀ state. As a result main fluorescence ($\Phi_f = 0.12$) at 22470 cm⁻¹ (445 nm) originates from the neutral DMAN, and minor one ($\Phi_f = 0.03$) at around 30000 cm⁻¹ (333 nm) from DMANH⁺ as shown in Figure 1c. The broad fluorescence band at 22470 cm⁻¹ (445 nm) shows very large Stokes shift (11000 cm⁻¹), which can be explained in terms of intramolecular charge-transfer character of the fluorescent ¹L_a state which leads to significant polarization stabilization in polar media.^{11–13,20} At pH 9.85, DMAN is expected to exist predominantly as the neutral form both in the *S*₀ and *S*₁ states (see Figure 1d). In fact, the absorption and fluorescence spectra show exclusively the feature of the neutral form. At pH 3.03 (Figure 1b), the absorption spectrum is almost identical with that obtained at

TABLE 1: Fluorescence Lifetime and Fluorescence Quantum Yield of DMAN and DMANH⁺ in Aqueous Solution with Different pH Values at 293 K

pH	DMANH ⁺		DMAN	
	τ_f^a (ns)	Φ_f	τ_f^b (ns)	Φ_f
1.02	32.7	0.56		<0.01
3.28	32.9	0.42	32.6	0.07
5.83		0.03	6.31	0.12
9.85		<0.01	6.25	0.13

^a Monitored at 340 nm. ^b Monitored at 450 nm.

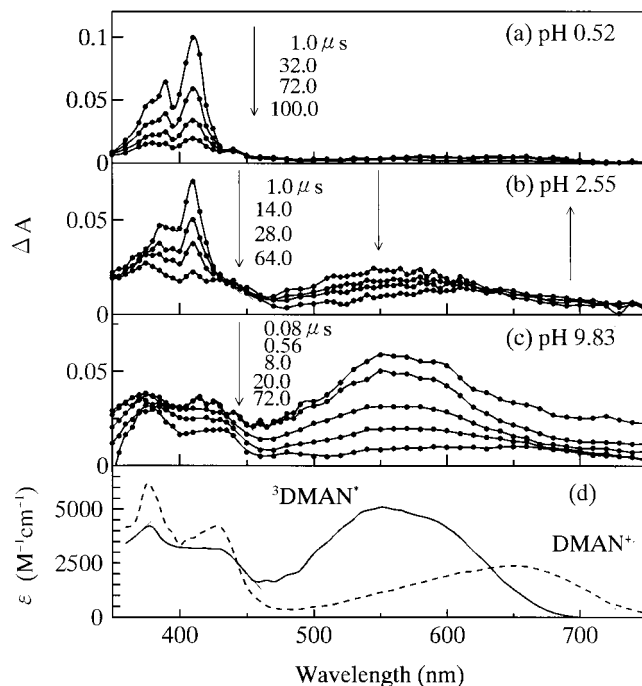


Figure 2. Transient absorption spectra obtained upon 266 nm laser photolysis of DMAN in aqueous solution at (a) pH 0.52, (b) pH 2.55, and (c) pH 9.83 at 293 K; (d) absorption spectra of ³DMAN* (—) and DMAN⁺* (---) from ref 9(b).

pH 1.02, indicating that at pH 3.03 most of the DMAN molecules in the ground state are protonated to produce DMANH⁺. However, the fluorescence spectra taken at 266 nm excitation (Figure 1b) exhibit two fluorescence bands (longer and shorter wavelengths) originating from the *S*₁ states of DMAN and DMANH⁺, respectively. The fluorescence excitation spectra monitored at 325 and 445 nm agreed well with the absorption spectrum of DMANH⁺, indicating that the partial proton dissociation occurred in the *S*₁ state of DMANH⁺ to give the fluorescence of DMAN.

The fluorescence lifetime (τ_f) and fluorescence quantum yield (Φ_f) of DMAN in aqueous solution are listed in Table 1. The τ_f values of DMAN in neutral and basic aqueous solutions are obtained to be ~ 6.3 ns, while that of the fluorescence band at 445 nm at pH 3.28 is obtained to be 32.6 ns which is very close to that (32.9 ns) for DMANH⁺ monitored at 325 nm at pH 3.28. This fact suggests that the decay rate of ¹DMAN* at pH 3.28 is determined by the proton dissociation rate ($9.6 \times 10^6 \text{ s}^{-1}$)⁷ from ¹DMANH⁺* according to consecutive reaction kinetics.

3.2. Transient Absorption Spectra. Figure 2 shows the time-resolved transient absorption spectra obtained by 266 nm laser flash photolysis of DMAN in degassed aqueous solution with different pH values, and the reference spectra of ³DMAN* and DMAN⁺*. Figure 3 shows those of the corresponding aerated systems. The transient absorption spectra obtained at pH 0.52 (Figure 2a) give the main absorption band at around 410 nm.

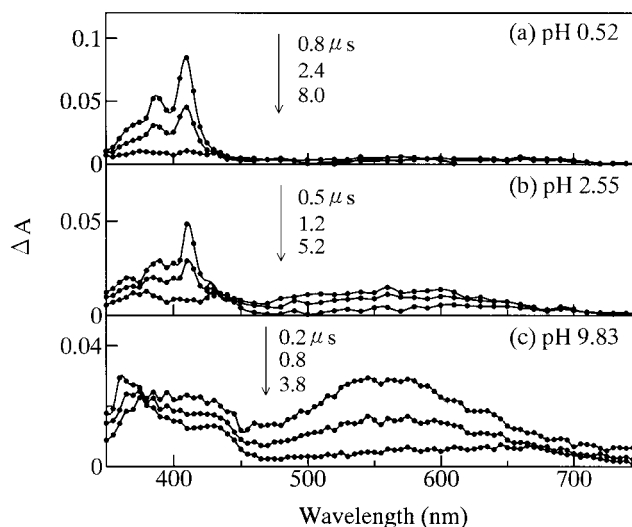
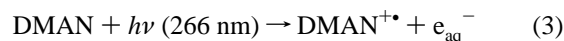


Figure 3. Transient absorption spectra obtained upon 266 nm laser photolysis of DMAN in aerated aqueous solution (a) pH 0.52, (b) pH 2.55, and (c) pH 9.83 at 293 K.

Under this condition, DMAN is protonated at the nitrogen atom both in the *S*₀ and *S*₁ states. From the pK_a^T value ($= 2.7$)⁸ of the excited triplet state, it can be expected that DMAN is protonated in the *T*₁ state as shown in Scheme 1. Actually, the spectral feature of the transient absorption spectra is very similar to that of the *T*_n ← *T*₁ absorption spectrum of 1-methylnaphthalene,²¹ and a typical quenching by dissolved oxygen is observed for this band (Figure 3a). Thus, the transient absorption band obtained at around 410 nm can be ascribed to the *T*_n ← *T*₁ absorption of DMANH⁺. The absorbance of ³DMANH⁺* decreased according to the first-order kinetics, with a lifetime of 25.6 μs at pH 0.52.

Under the basic condition (pH 9.83), broad absorption bands appear at around 550 and 720 nm as shown in Figure 2c. The first component can be assigned to the *T*_n ← *T*₁ absorption of DMAN from the spectral feature⁹ (see Figure 2d). The lifetime of ³DMAN* under this condition is obtained to be 15.6 μs. The second component with the absorption maximum at around 720 nm can be assigned to the hydrated electron (e_{aq}^-) from the characteristic spectral shape,²² and the facts that the absorption was quenched by dissolved oxygen and electron acceptors such as Eu³⁺. In the aerated system at pH 9.83 (Figure 3c), a broad absorption band with a maximum at 650 nm can be seen after disappearance of ³DMAN*. Judging from its spectral shape, this long-life component can be assigned to the DMAN cation radical (DMAN⁺*).⁹ These results demonstrate that DMAN in basic aqueous solution is photoionized upon 266 nm laser excitation, resulting in the formation of DMAN⁺* and e_{aq}^- :



As shown in Figure 4, the initial concentration of DMAN⁺* exhibits a linear laser power dependence under the laser pulse energies of $\leq 15 \text{ mJ pulse}^{-1} \text{ cm}^{-2}$, indicating that the photoionization of DMAN in basic aqueous solution takes place via one-photon absorption process. This photoinduced electron-ejection process from DMAN to solvent will be discussed in Section 3.3.

At pH 2.55, the prototropic equilibrium of DMAN in the *S*₀ state shifts to the protonated form, while in the excited states, proton dissociation occurs both in the *S*₁ and *T*₁ states to produce ¹DMAN* and ³DMAN*. The transient absorption spectrum at $t = 1.0 \mu\text{s}$ in Figure 2b is comprised of the *T*_n ← *T*₁ absorption

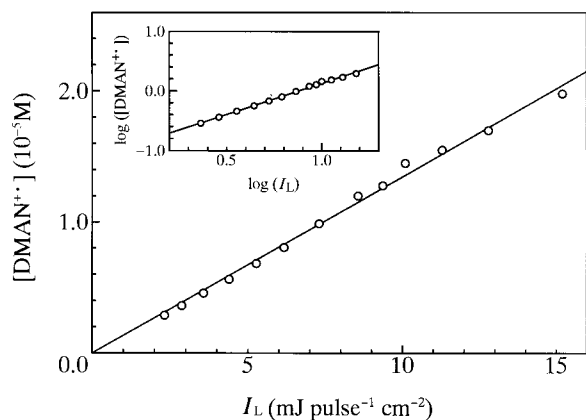


Figure 4. Laser power (I_L) dependence of the DMAN cation radical concentration generated by 266 nm laser photolysis of DMAN in aqueous solution at pH 9.83. Inset: its log–log plots.

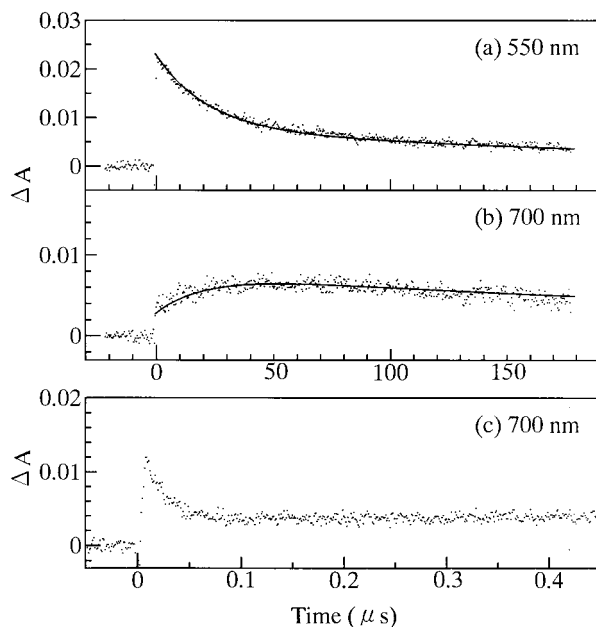


Figure 5. Time traces of the transient absorption spectra of DMAN in acidic aqueous solution (pH 2.55) monitored at (a) 550 nm and (b) 700 nm; (c) early time range at 700 nm.

bands due to ${}^3\text{DMAN}^*$ and ${}^3\text{DMANH}^{+*}$. In contrast to the S_1 state, the acid–base equilibrium should be established in the T_1 state because of the longer lifetime of the T_1 states. In fact, the observed lifetime (23 μs) of ${}^3\text{DMANH}^{+*}$ at pH 2.55 is very close to that for ${}^3\text{DMAN}^*$ (21 μs) under the same condition.

It is noteworthy in Figure 2b that at pH 2.55 the absorption band due to DMAN^{+*} appears at around 650 nm with decreasing of the absorption band due to ${}^3\text{DMAN}^*$ at 550 nm, and an isosbestic point is seen at around 640 nm. Figure 5, parts a and b, show the time traces of the transient absorption spectra in Figure 2b monitored at 550 and 700 nm, respectively. The time profile of the early time range at 700 nm is also displayed in Figure 5c. As shown in Figure 5c, the hydrated electron is very rapidly quenched by H_{aq}^+ , in consistent with the reported bimolecular rate constant of $2.3 \times 10^{10} \text{ M}^{-1} \text{ s}^{-1}$.^{23–25} Since the molar absorption coefficient of ${}^3\text{DMAN}^*$ at 700 nm is negligibly small compared to that of DMAN^{+*} (see Figure 2d), the time profile shown in Figure 5b can be regarded as time evolution of DMAN^{+*} . The time profile at 700 nm exhibits fast and slow rise components for DMAN^{+*} , suggesting that two different photoionization mechanisms are involved under this condition. The fast ionization process would take

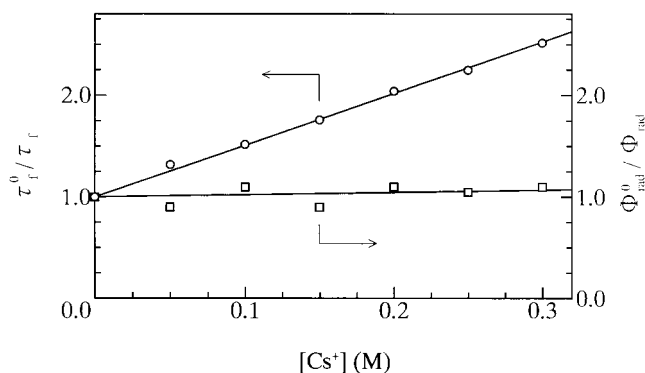


Figure 6. Plots of τ_f^0/τ_f (circles) and $\Phi_{\text{rad}}^0/\Phi_{\text{rad}}$ (squares) of DMAN as a function of $[\text{Cs}^+]$ in aqueous solution (pH 6.3) at 293 K.

TABLE 2: Quantum Yields for ${}^3\text{DMAN}^*$ and DMAN^{+*} in Aqueous Solution with Different pH Values at 293 K

pH	$\Phi({}^3\text{DMAN}^*)$	$\Phi_{\text{rad}}^{\text{S}}$ ^a	$\Phi_{\text{rad}}^{\text{T}}$ ^b	$\Phi_{\text{rad}}^{\text{c}}$
1.02	<0.01	<0.01	<0.01	<0.02
2.55	0.19	0.08	0.11	0.19
2.72	0.27	0.09	0.08	0.17
2.85	0.28	0.10	0.06	0.16
3.05	0.30	0.12	0.05	0.17
9.83	0.56	0.17	<0.01	<0.18

^a Yield of cation radical from singlet state. ^b Yield of cation radical from triplet state. ^c Total cation radical yield ($\Phi_{\text{rad}} = \Phi_{\text{rad}}^{\text{S}} + \Phi_{\text{rad}}^{\text{T}}$).

place from ${}^1\text{DMAN}^*$ produced by deprotonation of ${}^1\text{DMANH}^{+*}$. The slow rise time of DMAN^{+*} almost agrees with the decay time of ${}^3\text{DMAN}^*$ monitored at 550 nm (Figure 5a). In addition, the slow rise component at 700 nm disappeared in aerated water. Thus it appears that the slow ionization occurs from ${}^3\text{DMAN}^*$. Each photoionization mechanism will be discussed below.

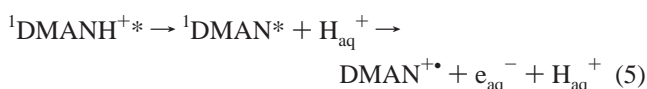
3.3. Direct Electron-Ejection from ${}^1\text{DMAN}^*$ to Water. In $\text{pH} \geq 6.0$ aqueous solutions, DMAN ejects an electron to solvent via one-photon absorption process upon 266 nm (4.66 eV) laser excitation (eq 3). To clarify whether the ionization takes place from the relaxed or nonrelaxed excited singlet state, we examined the effect of Cs^+ ion on the formation yield (Φ_{rad}) of DMAN^{+*} . The Cs^+ ion is known to be an effective singlet quencher in aqueous solution,^{26,27} where the quenching is usually caused by the external heavy atom effect, resulting in the enhancement of intersystem crossing. If the electron-ejection occurs from the relaxed S_1 state of DMAN, then the Φ_{rad} should decrease with increasing Cs^+ concentration ($[\text{Cs}^+]$). Figure 6 shows plots of τ_f^0/τ_f and $\Phi_{\text{rad}}^0/\Phi_{\text{rad}}$ as a function of $[\text{Cs}^+]$ for DMAN in aqueous solution at pH 6.2. Here τ_f and τ_f^0 are the fluorescence lifetimes of DMAN with and without Cs^+ and Φ_{rad} and Φ_{rad}^0 denote the quantum yields of the cation radical (DMAN^{+*}) formation with and without Cs^+ , respectively. From the following Stern–Volmer equation, the fluorescence quenching rate constant (k_q) was determined to be $8.1 \times 10^8 \text{ M}^{-1} \text{ s}^{-1}$:

$$\frac{\tau_f^0}{\tau_f} = 1 + k_q \tau_f^0 [\text{Cs}^+] \quad (4)$$

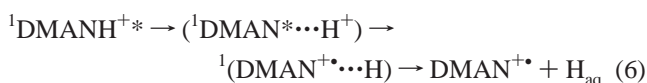
Nevertheless, the Φ_{rad} value was scarcely affected by addition of the Cs^+ ion. These results show that the electron-ejection of DMAN takes place mainly from the nonrelaxed S_1 (S_1^{\ddagger}) state. The ionization yields from ${}^1\text{DMAN}^*$ are listed in Table 2.

3.4. Electron-Ejection via ${}^1\text{DMANH}^{+\bullet}$ in Aqueous Solution. The time profile shown in Figure 5b exhibits two distinguishable (fast and slow) photoionization processes at pH 2.55, where most of DMAN molecules in the S_0 state are protonated on the nitrogen atom to produce DMANH^+ . The linear laser power (I_L) dependence was found for the fast photoionization process under the experimental conditions ($I_L < 15 \text{ mJ pulse}^{-1} \text{ cm}^{-2}$), indicating that the cation radical is produced by one-photon absorption process. Since DMANH^+ has a positive charge, the direct electron photoejection from DMANH^+ to produce its dication is not plausible. Here we propose three possible processes for the fast photoionization passing it through ${}^1\text{DMANH}^{+\bullet}$.

The first mechanism is the direct photoionization from the S_1^{\dagger} state of DMAN produced by photoexcitation of DMAN which is slightly populated in the ground state at pH 2.55. However, the possibility of this reaction is excluded by the following reasons: (1) the ϵ value of DMAN ($2600 \text{ M}^{-1} \text{ cm}^{-1}$) at 266 nm, which is about one-half compared to that of DMANH^+ ($5400 \text{ M}^{-1} \text{ cm}^{-1}$), (2) much lower population of DMAN than that of DMANH^+ , which can be estimated as $[\text{DMAN}]/[\text{DMANH}^+] \leq 0.01$ from the $\text{p}K_a$ value ($= 4.6$)⁷ at 293 K, and (3) the relatively small quantum yield ($\Phi_{\text{rad}}^0 < 0.18$) for the direct ionization in the S_1^{\dagger} state of DMAN in aqueous solution. The second mechanism is an electron-ejection to solvent from ${}^1\text{DMAN}^*$ which was produced by proton dissociation of ${}^1\text{DMANH}^{+\bullet}$:



The third mechanism is proton dissociation of ${}^1\text{DMANH}^{+\bullet}$ followed by electron transfer (ET) to H^+ as shown in the following equation:



In the first step, ${}^1\text{DMANH}^{+\bullet}$ releases a proton to produce ${}^1\text{DMAN}^*$ and H^+ in a solvent cage. In the second step, ET takes place from ${}^1\text{DMAN}^*$ to H^+ before completing hydration of H^+ to form a successor complex (${}^1(\text{DMAN}^{+\bullet\cdots}\text{H})$). Finally, the successor complex dissociates to form the products. The possibility of nongeminate ET reactions from free ${}^1\text{DMAN}^*$ to H_{aq}^+ in bulk water can be neglected, because their encounter probability should be significantly small at pH 2.55.

As shown in Figure 5c, one can see a fast decay component in the time profile observed at 700 nm. Since the spectral property and decay rate of the component agreed well with those of e_{aq}^- produced by photoionization of $\text{Fe}(\text{CN})_6^{4-}$ in water at pH 2.55, the fast decay component in Figure 5c can be assigned to e_{aq}^- . This finding suggests that the cation radical ($\text{DMAN}^{+\bullet}$) formation upon excitation of DMANH^+ is due, at least in part, to the second mechanism (eq 5).

To consider the contribution of the third mechanism, the Gibbs free energy change (ΔG^0) for the ET process between ${}^1\text{DMAN}^*$ and H^+ as shown in eq 7 was estimated by using electrochemical potentials:



The standard Gibbs free energy change of the hydrated H (H_{aq}), $\Delta G_{\text{f}}^0(\text{H}_{\text{aq}})$, is reported to be 222 kJ mol^{-1} ,²⁸ which corresponds to the Gibbs free energy change for the conversion ($\text{H}_{\text{aq}}^+ \rightarrow \text{H}_{\text{aq}}$) because of $\Delta G_{\text{f}}^0(\text{H}_{\text{aq}}^+) = 0$ convention. $\Delta G_{\text{f}}^0(\text{H}_{\text{aq}})$ includes

the hydration free energy change of hydrogen atom which is estimated to be 19 kJ mol^{-1} .^{28,29} In the calculations of ΔG^0 of the ET from ${}^1\text{DMAN}^*$ to H^+ in (${}^1\text{DMAN}^{\bullet\cdots}\text{H}^+$), the hydration free energy change of hydrogen atom can be neglected. Therefore the actual free energy change (ΔG^0) for the ET process in eq 7 can be estimated as follows:³⁰

$$\Delta G^0 = 96.5 \times E^0(\text{DMAN}^+/\text{DMAN})_{\text{aq}} - E_{\text{S}} + \Delta G_{\text{f}}^0(\text{H}) \quad (8)$$

where E_{S} is the $S_1 \leftarrow S_0$ transition energy of DMAN (319 kJ mol^{-1}), which can be estimated from the midpoint of the absorption and fluorescence spectra, $E^0(\text{DMAN}^+/\text{DMAN})$ is the oxidation potential of DMAN. The oxidation potential of DMAN in acetonitrile ($E^0(\text{DMAN}^+/\text{DMAN})_{\text{ACN}}$) is reported to be 0.75 eV ,³¹ which is corrected for difference in solvation energies in acetonitrile and in aqueous solution by using the following equation:^{32–34}

$$E^0(\text{DMAN}^+/\text{DMAN})_{\text{aq}} = E^0(\text{DMAN}^+/\text{DMAN})_{\text{ACN}} - \frac{(\Delta e)^2}{4\pi \epsilon_0 2r_{\text{D}}} \left[\frac{1}{\epsilon_{\text{ACN}}} - \frac{1}{\epsilon_{\text{H}_2\text{O}}} \right] \quad (9)$$

where, $E^0(\text{DMAN}^+/\text{DMAN})_{\text{aq}}$ is the oxidation potential of DMAN in aqueous solution, ϵ_0 is the dielectric constant in a vacuum, r_{D} is the radius of DMAN, and ϵ_{ACN} ($= 36.94$) and $\epsilon_{\text{H}_2\text{O}}$ ($= 80.16$) are the dielectric constants of acetonitrile and water.³⁵ The value of r_{D} was estimated from the density ($1.042 \times 10^3 \text{ kg m}^{-3}$)³⁶ of DMAN as 0.41 nm . Thus the $E^0(\text{DMAN}^+/\text{DMAN})_{\text{aq}}$ value is obtained to be 0.72 eV , and the overall free energy change for eq 7 is estimated to be -47 kJ mol^{-1} .

Judging from the exergonic nature of the process in eq 7, the third mechanism can also participate in the photoionization of DMAN. However, it is expected that the back electron-transfer reaction from H to $\text{DMAN}^{+\bullet}$ in ($\text{DMAN}^{+\bullet\cdots}\text{H}$), where ΔG^0 can be estimated to be -272 kJ mol^{-1} , would reduce the cation radical yield. Therefore, the ET reaction due to the third mechanism (eq 6) would be the minor process. The cation radical yields (Φ_{rad}) by the fast photoionization upon excitation of DMANH^+ in water with different pH values are listed in Table 2.

3.5. Ionization Process from ${}^3\text{DMAN}^*$ in Water. It seems reasonable to assume that the slow formation of $\text{DMAN}^{+\bullet}$ observed at pH 2.55 (Figure 5b) proceeds from the triplet state of DMAN (${}^3\text{DMAN}^*$), because the rise time of $\text{DMAN}^{+\bullet}$ (Figure 5b) is in agreement with the decay time of ${}^3\text{DMAN}^*$ (Figure 5a) and this process is not seen under the aerated condition (see Figures 2b and 3b). Recently, we have reported on occurrence of the ET reaction from the triplet state of DMB (${}^3\text{DMB}^*$) to the hydronium ion.⁴ Therefore, one can consider the possibility of the ET reaction between ${}^3\text{DMAN}^*$ and the hydronium ion for the slow formation mechanisms of $\text{DMAN}^{+\bullet}$. The lifetime of ${}^3\text{DMAN}^*$ ($21 \mu\text{s}$) at pH 2.55 is sufficiently long to form the encounter complex with H_{aq}^+ . To estimate the rate constant of the ET reaction from ${}^3\text{DMAN}^*$ to the hydronium ion, we made kinetic analyses on the time profile of the transient absorption spectra shown in Figure 2.

Since no significant absorbing species were recognized after disappearance of the DMAN cation radical and the hydrated electron, the overall absorbance changes ($\Delta A(t)$) of the transient absorption spectra of DMAN in acidic aqueous solution monitored at 550 nm can be expressed by the following

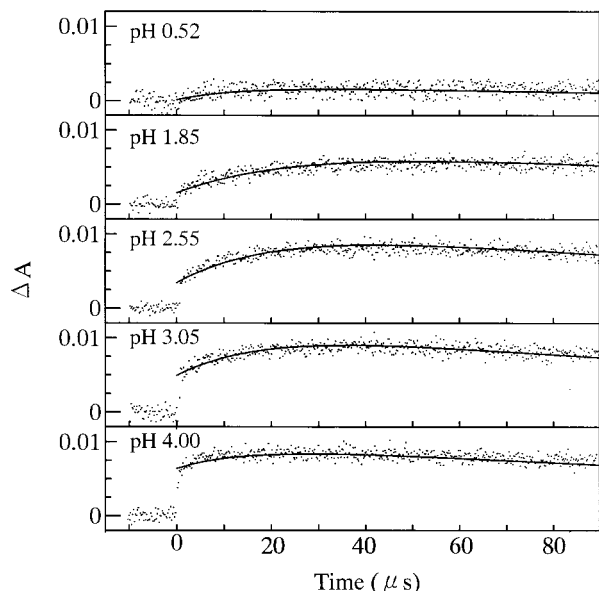


Figure 7. Time traces of the transient absorption spectra of DMAN monitored at 700 nm (a) pH 0.52, (b) pH 1.85, (c) pH 2.55, (d) pH 3.05, and (e) pH 4.00.

equation:

$$\begin{aligned} \Delta A_{550}(t) = & [{}^3\text{DMAN}^*]_{\text{max}} \epsilon_{\text{T}}^{550} \exp(-k_{\text{T}}^{\text{obs}} t) \\ & + [{}^3\text{DMAN}^*]_{\text{max}} \phi_{\text{ET}} \epsilon_{\text{rad}}^{550} \{ \exp(-k_{\text{rad}} t) - \\ & \exp(-k_{\text{T}}^{\text{obs}} t) \} \\ & + [\text{DMAN}^{+\bullet}]_0 \epsilon_{\text{rad}}^{550} \exp(-k_{\text{rad}} t) \\ & + [e_{\text{aq}}^-]_0 \epsilon_{\text{HE}}^{550} \exp(-k_{\text{HE}} t) \end{aligned} \quad (10)$$

where $k_{\text{T}}^{\text{obs}}$ and k_{rad} are the decay rate constants of ${}^3\text{DMAN}^*$ and $\text{DMAN}^{+\bullet}$, respectively (here k_{rad} was estimated to be $3.0 \times 10^3 \text{ s}^{-1}$ from the slow decay component in Figure 5a), ϕ_{ET} is the efficiency of the ET reaction from ${}^3\text{DMAN}^*$ to the hydronium ion, and ϵ_{T} and ϵ_{rad} are the molar absorption coefficients of ${}^3\text{DMAN}^*$ and $\text{DMAN}^{+\bullet}$, respectively. The ϵ_{T} value at 550 nm has been reported as $5100 \text{ M}^{-1} \text{ cm}^{-1}$.⁹ The ϵ_{rad} values at 550 and 700 nm can be determined to be 1140 and $1370 \text{ M}^{-1} \text{ cm}^{-1}$ by using the reported ϵ value of $\text{DMAN}^{+\bullet}$ ($2400 \text{ M}^{-1} \text{ cm}^{-1}$ at 650 nm) and its spectral shape.⁹ k_{HE} is the decay rate constant of e_{aq}^- in acidic aqueous solution, which is represented by $k_{\text{HE}} = k_{\text{HE}}^0 + k_{\text{HE}}' [\text{H}_3\text{O}^+]$. The bimolecular rate constant (k_{HE}') between e_{aq}^- and H_{aq}^+ has been reported as $2.3 \times 10^{10} \text{ M}^{-1} \text{ s}^{-1}$.^{23–25} $[\text{DMAN}^{+\bullet}]_0$ is the initial concentration of $\text{DMAN}^{+\bullet}$ produced from the S_1 state, and the value was determined by the initial absorbance of $\text{DMAN}^{+\bullet}$ at 700 nm. $[{}^3\text{DMAN}^*]_{\text{max}}$ is the maximum concentration of ${}^3\text{DMAN}^*$, which was obtained by subtracting the absorbance of $\text{DMAN}^{+\bullet}$ from the maximum absorbance at 550 nm. Since the lifetime ($2.8 \times 10^{-8} \text{ s}$) of e_{aq}^- at pH 2.55 is sufficiently short ($\leq 30 \text{ ns}$), the contribution of e_{aq}^- to the time profiles shown in Figure 5, parts a and b, can be neglected. The solid curves in Figure 5, parts a and b, were obtained by fitting eq 10 to the experimental values, where $k_{\text{T}}^{\text{obs}}$ and ϕ_{ET} were used as fitting parameters. The best-fitted values for $k_{\text{T}}^{\text{obs}}$ and ϕ_{ET} were $4.8 (\pm 0.2) \times 10^4 \text{ s}^{-1}$ and $0.45 (\pm 0.3)$, respectively.

Figure 7 shows time traces of the transient absorption spectra of DMAN monitored at 700 nm in degassed aqueous solution with different pH values. The time traces are found to change depending on the hydronium ion concentrations. The proportion of the fast rise component, i.e., fast ionization through proton

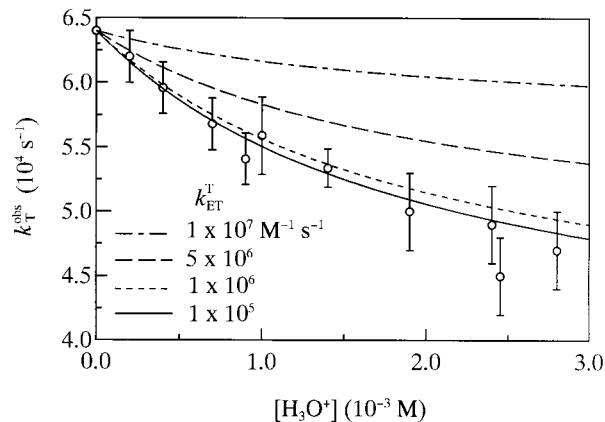
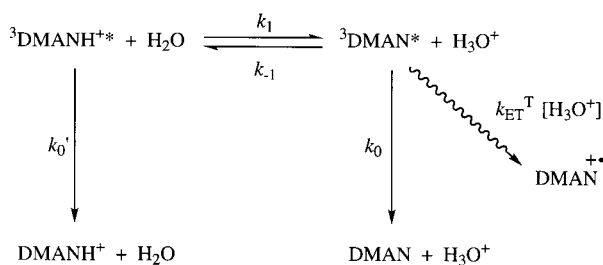


Figure 8. Plots of $k_{\text{T}}^{\text{obs}}$ as a function of $[\text{H}_3\text{O}^+]$. Curves were calculated by eq 11 using k_{ET}^{T} as a parameter.

SCHEME 2



dissociation of ${}^1\text{DMANH}^{+\bullet}$ decreases with an increase in the hydronium ion concentration. At pH 0.52, most of molecules in the S_1 state are protonated due to the relatively large bimolecular rate constant ($3.0 \times 10^9 \text{ M}^{-1} \text{ s}^{-1}$)⁷ for proton association compared with the proton dissociation rate constant ($9.6 \times 10^6 \text{ s}^{-1}$),⁷ resulting in the decrease in the fast photoionization yield.

To determine the rate constant for the bimolecular ET reaction (k_{ET}^{T}) from ${}^3\text{DMAN}^*$ to H_{aq}^+ , the $k_{\text{T}}^{\text{obs}}$ values were measured at various $[\text{H}_3\text{O}^+]$ values. Figure 8 shows plots of $k_{\text{T}}^{\text{obs}}$ as a function of $[\text{H}_3\text{O}^+]$ for aqueous DMAN at 293 K. The $k_{\text{T}}^{\text{obs}}$ value decreases with an increase of $[\text{H}_3\text{O}^+]$ suggesting that the equilibrium between ${}^3\text{DMANH}^{+\bullet}$ and ${}^3\text{DMAN}^*$ should be taken into account to estimate the value of k_{ET}^{T} . Hence, a relaxation scheme for ${}^3\text{DMAN}^*$ is assumed as shown in Scheme 2.

According to Scheme 2, the k_{ET}^{T} value can be expressed by eq 11:⁷

$$k_{\text{T}}^{\text{obs}} = \frac{k_0 + k_{\text{ET}}^{\text{T}} [\text{H}_3\text{O}^+] + k_0' K^{-1} [\text{H}_3\text{O}^+]}{1 + K^{-1} [\text{H}_3\text{O}^+]} \quad (11)$$

where k_0 and k_0' stand for the decay rate constant of ${}^3\text{DMAN}^*$ to the ground DMAN and that of ${}^3\text{DMANH}^{+\bullet}$ to the ground DMANH^+ , respectively. The k_0 and k_0' values were obtained as $6.4 \times 10^4 \text{ s}^{-1}$ and $3.9 \times 10^4 \text{ s}^{-1}$ by using solutions with pH 9.83 and 0.52, respectively, $K (= k_1/k_{-1})$ denotes an equilibrium constant between ${}^3\text{DMAN}^*$ and ${}^3\text{DMANH}^{+\bullet}$, which was estimated to be $2.0 \times 10^{-3} \text{ M}$ from $\text{p}K_{\text{a}}^{\text{T}}$ of the excited triplet state ($\text{p}K_{\text{a}}^{\text{T}} = 2.7$).⁸

The curves in Figure 8 were obtained on the bases of eq 11 by assuming different k_{ET}^{T} values. When the k_{ET}^{T} values are larger than $1 \times 10^6 \text{ M}^{-1} \text{ s}^{-1}$, then the fitting curves deviate significantly from the experimental values, while if we assumed k_{ET}^{T} values smaller than $1 \times 10^5 \text{ M}^{-1} \text{ s}^{-1}$, no apparent change was found for the calculated curves. Thus, the k_{ET}^{T} value was estimated to be less than $1 \times 10^5 \text{ M}^{-1} \text{ s}^{-1}$.

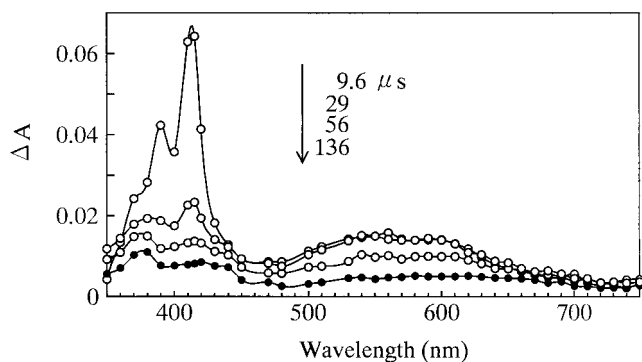


Figure 9. Transient absorption spectra obtained upon 266 nm laser photolysis of the Np-DMAN system in H₂O-ACN (4:1 v/v).

The results of the above kinetic analysis are supported by thermochemical considerations. In analogy with the thermochemical treatment on the reaction in the S₁ state of DMAN, we can consider the reaction between ³DMAN* and H_{aq}⁺ to produce DMAN^{+•} and a hydrogen atom:⁴



The ΔG^0 value for the reaction in eq 12 can be estimated by using eq 13:

$$\begin{aligned} \Delta G^0 &= 96.5 \times E^0(\text{DMAN}^+/\text{DMAN})_{\text{aq}} - E_{\text{T}} + \Delta G_{\text{f}}^0(\text{H}) \\ &= 47 \text{ kJ mol}^{-1} \end{aligned} \quad (13)$$

Here the E_{T} value represents the triplet energy of DMAN (226 kJ mol⁻¹) which was determined from the phosphorescence spectra of DMAN in ethanol: methanol (1:1 v/v) glass at 77 K. Thus, the ΔG^0 value for the reaction in eq 13 is evaluated as 47 kJ mol⁻¹. The highly endergonic nature of the ET reaction between ³DMAN* and the hydronium ion implies that the ET reaction in eq 12 cannot be a dominant mechanism.

Another possible mechanism for the slow formation of DMAN^{+•} from ³DMAN* is an electron-ejection process to solvent water. The possibility of the slow electron-ejection from ³DMAN* to solvent was examined by energy transfer experiments from triplet naphthalene (the triplet energy of Np: 255 kJ mol⁻¹)³⁵ to the ground DMAN. Figure 9 shows the transient absorption spectra obtained by 266 nm laser photolysis of the Np (1.0 × 10⁻⁴ M)-DMAN (1.3 × 10⁻⁵ M) system in H₂O-ACN (4:1 v/v). The structured absorption band at around 410 nm observed at a delay time of 9.6 μs is ascribable to the T_n ← T₁ absorption of Np.¹⁷ Since the direct excitation of the ground DMAN is negligible under the present experimental condition, the broad 550 nm band can be assigned to ³DMAN* produced by energy transfer from ³Np* to DMAN. After the decay of the broad 550 nm band, a red-shifted broad absorption band at 650 nm is seen which can be ascribed to DMAN^{+•} from its spectral shape.⁹ Since the electron-ejection efficiency would be reduced in H₂O-ACN (4:1 v/v) mixed solvent compared with that in H₂O, one cannot see isosbestic point in Figure 9. This finding supports the occurrence of the slow electron-ejection from ³DMAN* to water with a time constant of ca. 30 μs (see Figure 9).

In general, the ionization threshold of a solute molecule in water is significantly lowered compared with that in the gas phase.³⁸⁻⁴³ The ionization potential (IP_{liq}) of a solute molecule in the liquid phase can be estimated by the following equation:

$$\text{IP}_{\text{liq}} = \text{IP}_{\text{gas}} + P_+ + V_0 \quad (14)$$

where IP_{gas} is the ionization potential of a solute molecule in the gas phase, P₊ is the adiabatic electronic polarization energy of the medium by the positive ion, and the V₀ is the minimum energy of a quasi-free electron in the liquid phase relative to that of an electron in the gas phase. The IP_{gas} value of DMAN has been reported to be 7.00 eV.⁴⁴ The V₀ value in liquid water is known to be -1.2 eV.⁴⁵ In a theoretical model regarding solvents as the dielectric continuum, the value of P₊ can be estimated from the Born's expression:⁴⁶

$$P_+ = -\frac{e^2}{2r_+} \left(1 - \frac{1}{\epsilon_{\text{op}}} \right) \quad (15)$$

where e , r_+ , and ϵ_{op} are the electronic charge, effective ionic radius, and optical dielectric constant of the solvent, respectively. The polarization energy (P₊) calculated by eq 15 corresponds to fast electron photoejection processes in which orientational relaxation is not included. However, in slow photoionization processes of a solute molecule in water, the orientational relaxation should be included. Therefore, one can use the static dielectric constant (ϵ_{r}) instead of ϵ_{op} . In a similar manner, the free energy change for electron hydration (-1.67 eV)⁴⁷ can be used instead of V₀ for quasi-free electron. By using these values and $r_+ = 0.41$ nm as stated in Section 3.4, the IP_{liq} value of DMAN in aqueous solution is calculated to be 3.57 eV which is still ~1 eV larger than the triplet energy (2.34 eV) of DMAN. The difference in the calculated IP_{liq} and the triplet energy of DMAN suggests the presence of the other factors which stabilize the products. The solvent effects of water on the photoionization of aromatic amines involve not only general effects originating from the dispersion force but also the so-called specific effect which is usually caused by local interactions for the product cation radical. In fact, the photoionization yield of aniline derivatives in aqueous solution showed a good correlation with an extent of charge localization in the cation radical state rather than the magnitude of IP_{gas}.² According to MO calculations, the formal charge on the nitrogen atom of DMAN^{+•} was +0.450. This charge localization of the cation radical would be related to large stabilization of DMAN^{+•} in water. Recently, Neusser et al.⁴⁸ have reported that the dissociation energy (4790 cm⁻¹) of the indole-H₂O complex in the ground cation radical state was almost 3-fold as large as that obtained in the neutral state (1632 cm⁻¹) in the gas phase, due to enhancement of the hydrogen bonding in the ionic state caused by the additional charge-dipole interaction. Similar interactions between DMAN^{+•} and solvent water would be involved in the slow electron-ejection of DMAN.

It is of interest to compare the ionization in the triplet state of DMAN in water with that of 1,4-dimethoxybenzene (DMB) having a symmetric conformation. The slow electron-ejection from triplet DMB (³DMB*) to water has scarcely been observed.⁴ This may be due to the inefficient polarization stabilization because of the lack of charge localization in the cation radical (DMB^{+•}) in contrast to the case of DMAN^{+•}. However, the ET reaction from ³DMB* to the hydronium ion occurred efficiently with a rate constant of 7.5 × 10⁶ M⁻¹ s⁻¹, whereas that from ³DMAN* to the hydronium ion was not significant (≤ 1.0 × 10⁵ M⁻¹ s⁻¹). The former ET reaction may proceed via the triplet exciplex between ³DMB* and the hydronium ion, just like the proton-induced electron transfer via the triplet exciplex.^{49,50} For the latter ET reaction is restricted since the triplet exciplex between ³DMAN* and the hydronium ion may not be so stable because of the interaction of the nitrogen atom in ³DMAN* with protons to produce ³DMANH^{+•}. Thus, one can conclude that the electronic

structures both in the triplet state of the aromatic compounds and the product cation radical seem to control the ionization processes in the triplet state in water.

4. Concluding Remarks

The photoionization processes of DMAN in aqueous solution with different pH values at 293 K have been investigated by means of the nanosecond laser flash photolysis method at 266 nm and fluorescence spectroscopy. It was found that the ionization processes in the excited states of DMAN are quite different from those of DMB,^{3,4} and the following concluding remarks can be drawn.

(1) The photoionization reaction of DMAN is scarcely observed in the pH region < 1; that is, no photoionization takes place from DMANH⁺ to water.

(2) Under basic and neutral conditions, the electron-ejection occurs mainly from the nonrelaxed S₁ state (S₁[†]) of DMAN by one-photon absorption at 266 nm. This is due to the small IP_{iq} value of DMAN in aqueous solution resulting from appreciable polarization stabilization of the cation radical (DMAN^{†*}).

(3) In the pH range from ~2.0 to ~4.0, there are two possible ionization processes from both relaxed S₁ and T₁ states of DMAN, i.e., (a) the ET reaction from both the S₁ and T₁ states of DMAN to the hydronium ion, which is regarded as a minor process from thermochemical considerations, and (b) proton dissociation of the excited protonated DMAN (¹DMANH^{†*} and ³DMANH^{†*}) followed by electron-ejection to solvent water, which may be a more important process.

(4) It is found that the slow electron-ejection from ³DMAN* to water occurs with a time constant of ~30 μs.

(5) The localization of the formal charge on the nitrogen atom (+0.450) of the cation radical (DMAN^{†*}) plays an important role in the stabilization due to solvent reorientation in water.

(6) The difference in photoionization mechanisms between DMAN and DMB⁴ can be explained in terms of polarization stabilization of the product cation radical which is affected by charge localization in the cation state.

Acknowledgment. This work was supported by Grand-in-Aids for the Science Research from the Ministry of Education, Science, Sports and Culture of Japan (No. 11640496).

References and Notes

- (1) Saito, F.; Tobita, S.; Shizuka, H. *J. Chem. Soc., Faraday Trans.* **1996**, *92*, 4177.
- (2) Saito, F.; Tobita, S.; Shizuka, H. *J. Photochem. Photobiol. A: Chem.* **1997**, *106*, 119.
- (3) Grabner, G.; Monti, S.; Marconi, G.; Mayer, B.; Klein, C.; Köhler, G. *J. Phys. Chem.* **1996**, *100*, 20068.
- (4) Tajima, S.; Tobita, S.; Shizuka, H. *J. Phys. Chem. A* **1999**, *103*, 6097.
- (5) Shizuka, H. *Acc. Chem. Res.* **1985**, *18*, 141.
- (6) Arnaut, L. G.; Formosinho, S. J. *J. Photochem. Photobiol. A: Chem.* **1993**, *75*, 1.
- (7) Tsutsumi, K.; Shizuka, H. *Z. Phys. Chem. N.F.* **1978**, *111*, 129.
- (8) Jackson, G.; Porter, G. *Proc. R. Soc. London, Ser. A* **1961**, *260*, 13. The pK_a value of the triplet state of DMAN was determined by the method described in ref 8.
- (9) (a) Yamaji, M.; Kiyota, T.; Shizuka, H. *Chem. Phys. Lett.* **1994**, *226*, 199. (b) Kiyota, T.; Yamaji, M.; Shizuka, H. *J. Phys. Chem.* **1996**, *100*, 672.

- (10) Meech, S. R.; O'Connor, D. V.; Phillips, D. *J. Chem. Soc., Faraday Trans. 2* **1983**, *79*, 1563.
- (11) Suzuki, K.; Tanabe, H.; Tobita, S.; Shizuka, H. *J. Phys. Chem. A* **1997**, *101*, 4496.
- (12) Rückert, I.; Demeter, A.; Morawski, O.; Kühnle, W.; Tauer, E.; Zachariasse, K. A. *J. Phys. Chem. A* **1999**, *103*, 1958.
- (13) Suzuki, K.; Demeter, A.; Kühnle, W.; Tauer, E.; Zachariasse, K. A.; Tobita, S.; Shizuka, H. *Phys. Chem. Chem. Phys.* **2000**, *2*, 981.
- (14) Eaton, D. F. *Pure Appl. Chem.* **1988**, *60*, 1107.
- (15) Perichet, G.; Chapelon, R.; Pouyet, B. *J. Photochem.* **1980**, *13*, 67.
- (16) Bebelaar, D. *Chem. Phys.* **1974**, *3*, 205.
- (17) Bonneau, R.; Carmichael, I.; Hug, G. L. *Pure Appl. Chem.* **1991**, *63*, 289.
- (18) Berlman, I. B. *Handbook of Fluorescence Spectra of Aromatic Molecules*; Academic Press: New York, 1965.
- (19) Birks, J. B. *Photophysics of Aromatic Molecules*; John Wiley and Sons Ltd.: London, 1970.
- (20) Mataga, N. *Bull. Chem. Soc. Jpn.* **1963**, *36*, 654.
- (21) Carmichael, I.; Helman, W. P.; Hug, G. L. *J. Phys. Chem. Ref. Data* **1987**, *16*, 239.
- (22) (a) Hart, E. J.; Boag, J. W. *J. Am. Chem. Soc.* **1962**, *84*, 4090. (b) Boag, J. W.; Hart, E. J. *Nature* **1963**, *197*, 45. (c) Baxendale, J. H.; Fielden, E. M.; Capellos, C.; Francis, J. M.; Davies, J. V.; Ebert, M.; Gilbert, C. W.; Keene, J. P.; Land, E. J.; Swallow, A. J.; Nosworthy, J. M. *Nature* **1964**, *201*, 468.
- (23) Green, N. J. B.; Pilling, M. J.; Pimblott, S. M.; Clifford, P. *J. Phys. Chem.* **1990**, *94*, 251.
- (24) Goulet, T.; Jay-Gerin, J.-P. *J. Chem. Phys.* **1992**, *96*, 5076.
- (25) Elliot, A. J.; McCracken, D. R.; Buxton, G. V.; Wood, N. D. *J. Chem. Soc., Faraday Trans.* **1990**, *86*, 1539.
- (26) Zechner, J.; Köhler, G.; Grabner, G.; Getoff, N. *Chem. Phys. Lett.* **1976**, *37*, 297.
- (27) Lachish, U.; Ottolenghi, M.; Stein, G. *Chem. Phys. Lett.* **1977**, *48*, 402.
- (28) Han, P.; Bartels, D. M. *J. Phys. Chem.* **1990**, *94*, 7294.
- (29) Jortner, J.; Noyes, R. M. *J. Phys. Chem.* **1966**, *70*, 770.
- (30) Rehm, D.; Weller, A. *Isr. J. Chem.* **1970**, *8*, 259.
- (31) Zweig, A.; Maurer, A. H.; Roberts, B. G. *J. Org. Chem.* **1967**, *32*, 1322.
- (32) Weller, A. *Z. Phys. Chem. N.F.* **1982**, *133*, 93.
- (33) Schuster, G. B.; Yang, X.; Zou, C.; Sauerwein, B. *J. Photochem. Photobiol. A: Chem.* **1992**, *65*, 191.
- (34) Chen, P.; Mecklenburg, S. L.; Meyer, T. J. *J. Phys. Chem.* **1993**, *97*, 13126.
- (35) Murov, S. L. *Handbook of Photochemistry*; Marcel Dekker: New York, 1993.
- (36) Dean, A. J. *Lange's Handbook of Chemistry*; McGraw-Hill: New York, 1973.
- (37) Shizuka, H.; Hagiwara, H.; Fukushima, M. *J. Am. Chem. Soc.* **1985**, *107*, 7816.
- (38) *Photodissociation and Photoionization*; Yakovlev, B. S., Lukin, L. V., Lawley, K. P., Eds.; Wiley: New York, 1985.
- (39) Braun, C. L.; Scott, T. W. *J. Phys. Chem.* **1983**, *87*, 4776.
- (40) Lukin, L. V.; Tolmachev, A. V.; Yakovlev, B. S. *Chem. Phys. Lett.* **1983**, *99*, 16.
- (41) Hirata, Y.; Mataga, N.; *J. Phys. Chem.* **1985**, *89*, 4031.
- (42) Holroyd, R. A.; Preses, J. M.; Zevos, N. *J. Chem. Phys.* **1983**, *79*, 483.
- (43) García, C.; Smith, G. A.; McGimpsey, W. G.; Kochevar, I. E.; Redmond, R. W. *J. Am. Chem. Soc.* **1995**, *117*, 10871.
- (44) Maier, J. P. *Helv. Chim. Acta* **1974**, *57*, 994.
- (45) (a) Grand, D.; Bernas, A.; Amouyal, E. *Chem. Phys.* **1979**, *44*, 73. (b) Mialocq, J. C.; Amouyal, E.; Bernas, A.; Grand, D. *J. Phys. Chem.* **1982**, *86*, 3173.
- (46) Born, M. *Z. Physik.* **1920**, *1*, 45.
- (47) Conway, B. E. *Ionic Hydration in Chemistry and Biophysics*; Elsevier: New York, 1981.
- (48) Braun, J. E.; Grebner, Th. L.; Neusser, H. J. *J. Phys. Chem. A* **1998**, *102*, 3273.
- (49) Yamaji, M.; Sekiguchi, T.; Hoshino, M.; Shizuka, H. *J. Phys. Chem.* **1992**, *96*, 9353.
- (50) Shizuka, H. *Pure Appl. Chem.* **1997**, *69*, 825.